High-Throughput Optical Circuit Switch for Intra-Datacenter Networks Based on Spatial Super-Channels

Eiji Honda[1], Yojiro Mori[1], Hiroshi Hasegawa[1], Ken-ichi Sato[2]
[1]*Nagoya University, Furo-cho, Chikusa, Nagoya, 464-8603 Japan*
[2]*The National Institute of Advanced Industrial Science and Technology (AIST), 1-1-1 Umezono, Tsukuba, Ibaraki, 305-8568 Japan*
e_honda@nuee.nagoya-u.ac.jp

Abstract: We propose a novel optical circuit switch architecture based on spatial super-channels. We construct part of a 1,536×1,536 optical switch and its performance is experimentally confirmed. The total throughput of the switch reaches 2.1 Pbps.

1. Introduction

With the spread of video-streaming services and cloud-computing services, datacenter-related traffic is growing at 25% a year [1]. Intra-datacenter traffic accounts for over 70% of all datacenter-related traffic [1]. To process such large amounts of intra-datacenter traffic cost-effectively, optical switch networks or opto-electronic hybrid switch networks are being intensively studied [2–7]. Among various optical-switching technologies, the 3D microelectromechanical system (MEMS) is one candidate for inter-rack connection [2]. However, the available number of ports is limited to about 300. While the silicon-photonic planar 2D MEMS switch provides a small footprint, its available scale is very limited, 64×64 [8]. Another switch candidate is based on semiconductor optical amplifiers (SOAs) [9,10]; although this approach can realize compact and lossless switching, power consumption tends to be very high because of a large number of SOAs needed. Given this background, we previously proposed a large-scale optical circuit switch architecture that combines delivery-and-coupling (DC) planar space switches and wavelength-routing (WR) switches [4]. This scheme was successfully demonstrated as a 1,536×1,536 strictly non-blocking optical circuit switch with a 150 Tbps throughput [11]. In order to expand the total switch throughput, we need to extend the scale of the WR switch or that of the DC switch. The scale of WR switch is mostly limited by the available wavelength bandwidth of optical amplifiers. Increasing the DC-switch scale increases the signal power loss and hence the scale of this configuration is limited by the available transmitter power. In addition, the cost of the DC switch increases super-linearly against the throughput [4]. Thus, in the switch that combines DC switches with WR switches, the feasible switch throughput is limited.

In this paper, we propose a novel optical circuit switch based on spatial super-channels, which utilizes space-division multiplexing (SDM) in addition to the conventional combination of planar space switching and wavelength-routing switching. To confirm the technical feasibility of the proposed switch architecture, we construct part of a 1,536×1,536 optical switch; we use the DC-switch scale of 16, the WR-switch scale of 96, and evaluate its transmission characteristics with 96-wavelength 1.4 Tbps DP-16QAM signals comprising 7 spatial subchannels. The total throughput of the optical circuit switch reaches 2.1 Pbps (=16×96×1.4 Tbps).

2. Proposed Switch Architecture

Figure 1 is a schematic of the proposed switch architecture based on spatial super-channels. The switch consists of MN wavelength-tunable transmitters supporting N wavelengths and L spatial subchannels, LN $M\times M$ DC planar space switches comprising M $1\times M$ optical selectors and M $M\times 1$ optical couplers, LM $N\times N$ WR switches, and MN wavelength-fixed receivers supporting L spatial subchannels, where N represents the number of wavelengths and M denotes the scale of the DC switch. An $N\times N$ WR switch is composed of n $(N/n)\times 1$ couplers, n EDFAs, and an $n\times N$ uniform-loss and cyclic-frequency (ULCF) AWG. Figure 2 depicts an 8×8 WR switch using a 2×8 ULCF AWG as an example. Using $n\times N$ ULCF AWGs instead of $1\times N$ AWG decreases the degree of couplers for signal aggregation by n i.e., WR switch loss is reduced [11].

The switching operation is as follows: L subchannel signals are generated from a transmitter supporting N wavelengths, where the wavelength is assigned according to the target receiver. The L subchannel signals are then input to L single-core fibers or an L-core fiber. After transmission, the L subchannel signals are jointly directed by L $M\times M$ DC switches and sent to L WR switch parts. In each space layer, multiple wavelength signals are aggregated by an $(N/n)\times 1$ coupler and amplified by an EDFA; the wavelength signals are then demultiplexed by an $n\times N$ ULCF AWG. Finally, the target signal comprising L subchannels is detected by the target receiver. It should be noted that the skews among spatial subchannels can easily be offset by digital buffers in the receiver; no complicated MIMO processing is necessary since we do not consider the use of coupled-core fibers and multi-mode fibers. This switch configuration also obviates the use of immature SDM devices, e.g. the multicore EDFA.

By introducing spatial super-channels to the proposed optical switch, the switch throughput can be increased without increasing the DC-switch scale. Table 1 summarizes the number of switch elements necessary for constructing the switch in each switch configuration. In the proposed architecture, the hardware cost increases linearly with the throughput, i.e., the cost per bit does not increase against the throughput.

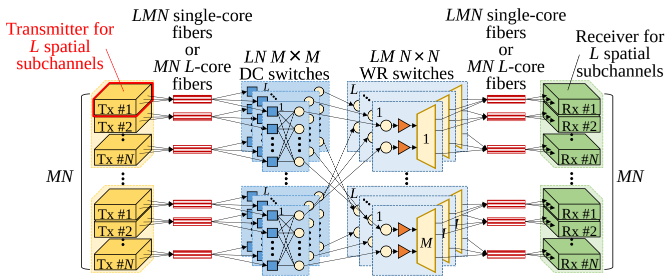

Fig. 1. Proposed switch architecture using spatial super-channels.

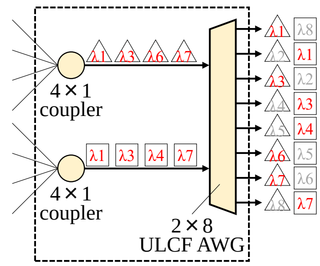

Fig. 2. 8×8 WR switch using a 2×8 ULCF AWG.

Table 1. The numbers of switch elements necessary for constructing an $MN \times MN$ switch, where the proposed architecture offers L times greater throughput than the conventional one. B denotes bps of a (sub)channel.

	Conventional (throughput: *MNB*) [11]			Proposed (throughput: *LMNB*)		
	Total	Per-port	Per-bps	Total	Per-port	Per-bps
Number of DC switches	N	$1/M$	$1/MB$	LN	L/M	$1/MB$
Number of 1×2 selectors*	$NM(M-1)$	$M-1$	$(M-1)/B$	$LNM(M-1)$	$L(M-1)$	$(M-1)/B$
Number of EDFAs	M	$1/N$	$1/NB$	LM	L/N	$1/NB$
Number of AWGs	M	$1/N$	$1/NB$	LM	L/N	$1/NB$

*An $M \times M$ DC switch includes $M(M-1)$ 1×2 selectors.

3. Simulations

We evaluate the attainable maximum switch scale via computer simulations. The modulation format is 100 Gbps DP-QPSK or 200 Gbps DP-16QAM for each (sub)channel. We assume 96 wavelengths aligned on the 50-GHz grid in the full C-band. The number of spatial subchannels and transmitter output power are parameterized. The signals are sent to an $M \times M$ DC planar space switch over a transmission link with a 3.5 dB loss including the connection loss. The loss of the $M \times M$ DC switch is set to ceil($\log_2 M$)×4 dB including the excess loss, where ceil( ) denotes the ceiling function. After multiple signals are aggregated by an 8×1 coupler and amplified by an EDFA, the multiplexed signal passes through a 1×2 splitter and a pair of 12×48 ULCF AWGs. Here, we adopt a pair of interleaved ULCF AWGs to reduce the impact of frequency deviation [11]. The losses of the 8×1 coupler, the 1×2 splitter, and the 12×48 ULCF AWG are set to 10.5 dB, 3.5 dB, and 9 dB, respectively. The noise figure and saturation power of the EDFA are 5 dB and 20 dBm, respectively. The target bit-error ratio (BER) is set to 10^{-2}. Figures 3(a) and (b) show the maximum overall switch scales against transmitter power per subchannel, where a 100 Gbps DP-QPSK signal and 200 Gbps DP-16QAM signal are used, respectively, as a (sub)channel. In both cases, the required transmitter power per subchannel against the port count is the same regardless of the number of spatial subchannels, L; i.e., the required transmitter power per bps does not change even though L is increased to enlarge the throughput. When the transmitter power is 0 dBm and L is 7, the attainable port count is 1,536×1,536 for 1.4 Tbps DP-16QAM signals.

4. Experiments

To confirm the technical feasibility of the proposed switch, we constructed part of a 1,536×1,536 optical circuit switch assuming 7 spatial subchannels for each channel. We used 7-core fibers to connect transponders to switch ports. We evaluated its transmission characteristics with 1.4 Tbps DP-16QAM signals comprising 7 spatial subchannels. We measured the BERs of 96 wavelengths in the full C-band. Figure 4 depicts the experimental setup. The target subchannel was generated by a transmitter, where the transmitter power per subchannel was set to 2 dBm considering the simulation results and a 2 dB margin. After passing through the 1-km 7-core fiber, the signal was input to part of a 16×16 DC planar space switch and delivered to a WR switch. Here, the loss of 7-core fiber was 3.5 dB including losses of fan-in and fan-out. In the WR switch, the signal was combined with 95 wavelength non-target signals as inter-band crosstalk via an 8×1 aggregation coupler. Then, the signals were amplified by an EDFA, where the losses of the DC switch and the aggregation coupler were compensated. The losses of the 16×16 DC switch and the 8×1 aggregation coupler were 16 dB and 10 dB, respectively. After loss compensation, signals were split by the 1×2 splitter and demultiplexed by a pair of interleaved 12×48 ULCF AWGs. Here, signals whose wavelength were the same as the target signal were input to the remaining input ports of ULCF AWGs as intra-band crosstalk. The extinction ratio of ULCF AWG ranged from 32 dB to 39 dB depending on input/output port and signal wavelength. Finally, the target signal was detected and demodulated by a digital coherent receiver. Figure 5 plots the measured BERs of all wavelengths in each core. We confirmed that all channels achieved BERs under the target value of 10^{-2}. The total throughput can reach 2.1 Pbps (=1,536×1.4 Tbps).

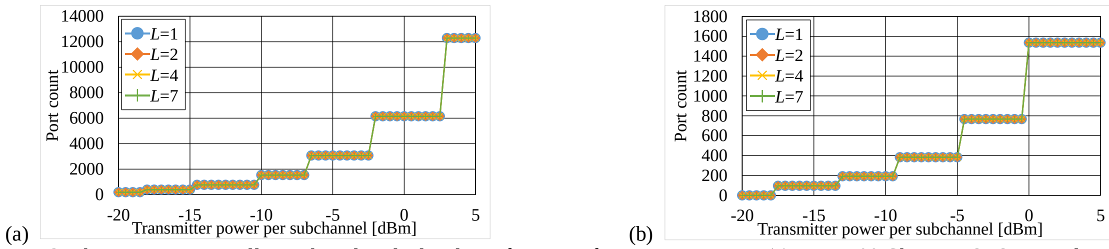

Fig. 3. The maximum overall switch scale calculated as a function of transmitter power; (a) using 100 Gbps DP-QPSK signals and (b) using 200 Gbps DP-16QAM signals. *L* represents the number of spatial subchannels.

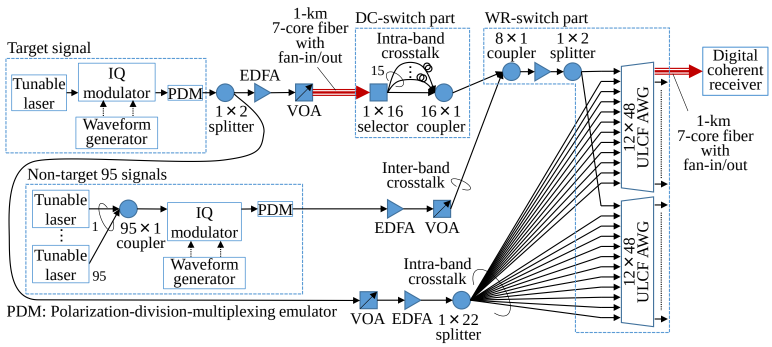

Fig. 4. Experimental setup.

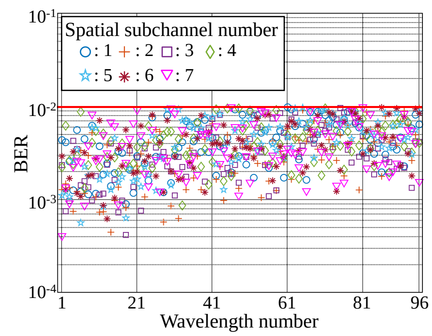

Fig. 5. Measured BERs.

5. Conclusion

We proposed a novel optical circuit switch architecture based on spatial super-channels; it utilizes SDM in addition to the conventional combination of planar space switching and wavelength-routing switching. To confirm the technical feasibility of the proposed switch architecture, we constructed part of a 1,536×1,536 optical switch and measured BERs of 1.4 Tbps DP-16QAM signals comprising 7 spatial subchannels. The total throughput of the switch was 2.1 Pbps.

Acknowledgment: This work was partly supported by the New Energy and Industrial Technology Development Organization (NEDO) and the Hibi Science Foundation.

6. References

[1] Cisco Systems, Inc., "Cisco global cloud index: forecast and methodology, 2016–2021 white paper," https://www.cisco.com/c/en/us/solutions/collateral/service-provider/global-cloud-index-gci/white-paper-c11-738085.html.
[2] N. Farrington et al., "Helios: a hybrid electrical/optical switch architecture for modular data centers," ACM SIGCOMM Comp. Commun. Rev. - SIGCOMM '10 **40**, 339-350 (2010).
[3] C. Kachris and I. Tomkos, "A survey on optical interconnects for data centers," IEEE Commun. Surv. Tutorials **14**, 1021-1036 (2012).
[4] K. Sato, "Realization and application of large-scale fast optical circuit switch for data center networking," IEEE/OSA J. Lightwave Technol. **36**, 1411-1419 (2018).
[5] F. Yan et al., "HiFOST: a scalable and low-latency hybrid data center network architecture based on flow-controlled fast optical switches," IEEE/OSA J. Opt. Commun. Netw. **10**, 1-14 (2018).
[6] K. Suzuki et al., "Low-insertion-loss and power-efficient 32 × 32 silicon photonics switch with extremely high-Δ silica PLC connector," IEEE/OSA J. Lightwave Technol. **37**, 116-122 (2019).
[7] R. Proietti et al., "Experimental demonstration of a 64-port wavelength routing thin-CLOS system for data center switching architectures," IEEE/OSA J. Opt. Commun. Netw. **10**, B49-B57 (2018).
[8] T. J. Seok el al., "Large-scale broadband digital silicon photonic switches with vertical adiabatic couplers," OSA Optica **3**, 64-70 (2016).
[9] M. Ding et al., "Hybrid MZI-SOA InGaAs/InP photonic integrated switches," IEEE J. Sel. Top. Quantum Electron. **24**, 1-8 (2018).
[10] Q. Cheng et al., "Demonstration of the feasibility of large-port-count optical switching using a hybrid Mach–Zehnder interferometer–semiconductor optical amplifier switch module in a recirculating loop," OSA Opt. Lett. **39**, 5244-5247 (2014).
[11] H. Nagai et al., "Design and verification of large-scale optical circuit switch using ULCF AWGs for datacenter application," IEEE/OSA J. Opt. Commun. Netw. **10**, 82-89 (2018).